NUMERICAL MODELLING OF THERMO-MECHANICAL EFFECTS DEVELOPED IN RESISTANCE SPOT WELDING OF E304 STEEL WITH COPPER INTERLAYER

D. C. Birsan, G. Simion*

"Dunarea de Jos" University of Galati, Faculty of Engineering, 47 Domneasca St., 800008, Galati, Romania
*Corresponding author's e-mail address: george.simion@ugal.ro

ABSTRACT

Resistance spot welding is a technique applied to join two or more similar or dissimilar metals, by applying pressure and electric current to the spot-weld area. Based on the electrical resistance property of metals, a great amount of heat is generated and used to carry out materials joints, by creating a molten metal nucleus between the components to be welded. The influence of an interlayer material, positioned between the parent materials, on the strength of similar or dissimilar welded joints was studied by researchers worldwide. In most cases, by optimising the process parameters, an increase in the welded joint strength was achieved. In this paper, the resistance spot welding of 1mm thick E304 stainless steel sheets, both with and without a copper foil interlayer, was investigated, by applying, in all cases, the same process parameters. The tensile test of the joints showed a decrease in the strength of joints performed with interlayer metal. A method to control the deterioration level of the joint' mechanical properties is the Finite Element Analysis which allows to optimise the process parameters so that the negative effects of the process on the joint quality to be limited. It was found that an increase in amperage is needed to compensate for the addition of the interlayer metal and to obtain an adequate melting in the spot-weld area. This modification causes an increase of the molten core diameter that will lead to improvement of the welded joint strength, while no significant influence on the internal stress level was noticed in the processing and numerical analysis of the output data.

KEYWORDS: *resistance spot welding, E304 stainless steel, Copper interlayer, finite element analysis.*

1. INTRODUCTION

Resistance spot welding (RSW) is widely used in the automotive and aeronautical industries. This type of welding uses a very high amount of current and a very low voltage. In general, thin sheets of similar or different metals can be welded by this process. Welding thicker sheets is generally difficult to do with RSW because the heat very easily dissipates into the surrounding metal mass.

The principle used in this study is defined by SR EN ISO 15614-12:2015. It means that the welding is done electrically by pressure. This is performed by passing electrical current through two or more pieces that are overlapped and tightened between the contact electrodes. The stages of the spot welding operation are as follows:

1. Overlapping the parts to be welded in the desired position between the electrodes;
2. Lowering the upper electrode by applying a pressing force in order to ensure electrical contact;
3. Connecting the electric current for a time long enough to create a core of molten metal between the parts. The duration can be from a few milliseconds to a few seconds;
4. The current is interrupted, and the pressure is maintained to avoid surface burns;
5. After the current interruption, the lifting of the upper electrode and releasing of the pressing force are delayed for a while to ensure the solidification of the molten core.

Researchers have analysed various aspects of simulation, modeling, and process optimization during resistance spot welding of steel [1]-[5]. In this work, the relationship between welding parameters, weld strength, and weld quality is analysed in detail. On the simulation side, each time step is solved based on electro-thermal, mechanical, and metallurgical analysis. In this article, the discussion focuses on modelling the electro-thermal coupling, the mechanical coupling being studied by other authors [6]-[8]. Most methods that simulate thermal contact by

Date of submission/acceptance: 24.10.2022/15.12.2022 https://doi.org/10.35219/awet.2022.07

finite element analysis consider thin layers of elements that model the contact properties.

In other methods, the electrical contact condition is to connect elements that are also facing each other or to connect the components with two nodes [8], [9]. In these cases, the relative displacement is not easy to explain due to the mechanical analysis during the welding process, and due to the limitation of this geometric assumption. This generates difficulties in meshing both the electrode and the sheet, and also the joining of the plates.

The RSW process involves strong interactions between the thermal, electrical, mechanical, and metallurgical domains. The schematic representation is presented in figure 1.

Contact definition is an important part of the finite element analysis of the RSW process. Contact properties have a significant impact on the simulation steps. The most important electrical and thermal parameters are electrical contact resistivity and thermal contact conductivity. These two important temperature-dependent parameters significantly affect the heat generation rate and the development of the molten metal core [23].

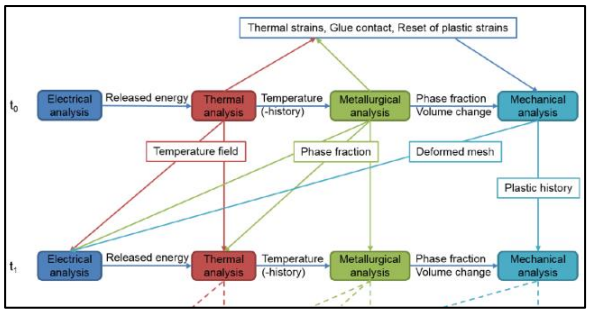

Fig. 1. Coupling analysis in welding simulation [10]

Applying Bay and Wanheim's relation, the electrical contact conductivity was automatically calculated when simulating the welding process with equation 2 [10].

$$q = 3 \cdot \left(\frac{\sigma_{soft}}{\sigma_n} \right) \cdot \left(\frac{\rho_1 + \rho_2}{2} \right) + \rho_c \qquad (2)$$

where:

- σ_{soft} - flow stress of the softer material (temperature dependent);
- σ_n - contact normal stress;
- ρ_1, ρ_2 - resistivity of the contact partners (temperature and phase-dependent);
- ρ_c - resistivity of coatings (optional).

The contact electrical resistance is 30 times larger than the material electrical resistance in most cases. During the welding process, the rise in temperature causes the electrical resistance of the material to increase, and due to the compression of the sheet, the contact resistance rapidly decreases. A graphical representation of this phenomenon is presented in figure 2.

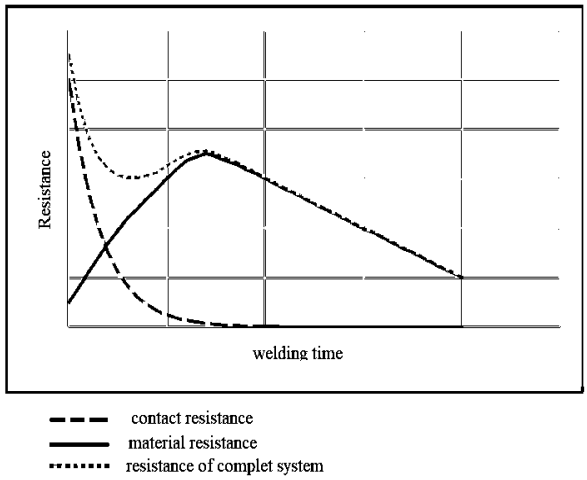

Fig. 2. Electrical resistances variation during the welding process [10]

Dissimilar materials, due to their chemical composition and different mechanical characteristics, raise certain challenges during welding [11]-[15]. In some studies, the researchers concluded that the introduction of an intermediate layer of Cu facilitates quality welds of dissimilar materials, through certain welding processes including electron beam welding [16], [17], arc welding [18], or diffusion welding [19].

The researchers also investigated the influence of adding an intermediate material in welding similar joints. Thus Roudbari, M et al. investigated the influence of using an intermediate layer of S1006 steel wires on the explosion welding of Al1050 aluminum plates [20]. Zhang, W investigated the influence of an intermediate layer of copper in ultrasonic spot welding NiTi alloy plates [21]. Dharaiya, V. et al. investigated the influence of intermediary layers of Cu and stainless steel SS304 on resistance spot welding AISI 1020 steel sheets [22].

In most of the studies, the tests lead to an increase in the joints' strength. For the other cases, it is necessary to optimize the parameters in order to take into account the influence on the welding process of the intermediate material.

This study investigates the influence of adding a copper foil interlayer on the mechanical characteristics of the joint when resistance spot welding E304 stainless steel sheets. This material is frequently used in the fabrication of appliances and commercial food processing equipment where resistance spot welding is employed.

The novelty of this paper consists in using finite element analysis for optimizing the welding parameters in order to compensate for the presence of the copper foil interlayer in the welded joints.

2. MATERIALS AND METHODS

2.1. Materials and Experiments

E304 stainless steel sheets and copper foils with the dimensions 80x25x1mm and 10x10x0.1mm were prepared for welding (Fig. 3, 4). Five samples of both combinations, stainless steel-stainless steel (SS-SS) and stainless steel-copper interlayer-stainless steel (SS-Cu-SS), were resistance spot welded on the manual machine with a pedal. The welding parameters are presented in table 1. The mechanical characteristics of E304 stainless steel are presented in table 2 and the chemical compositions of the materials used to form the welded joint are presented in table 3.

Table 1. Welding parameters for resistance spot welding

Current [A]	Force [N]	Time [s]
4000	1700	1.8

Table 2. Mechanical characteristics of E304 steel

Tensile Strength, Yield	Tensile Strength, Ultimate	Elongation
215 [MPa]	505 [MPa]	>45[%]

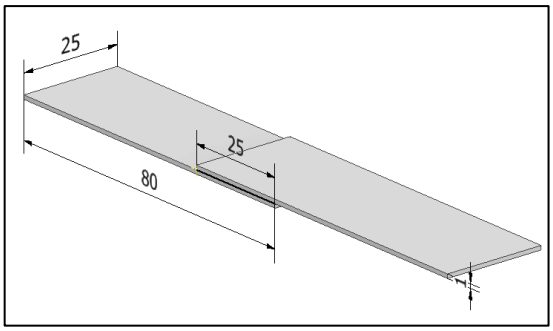

Fig. 3. Schematic representation of prepared sheets

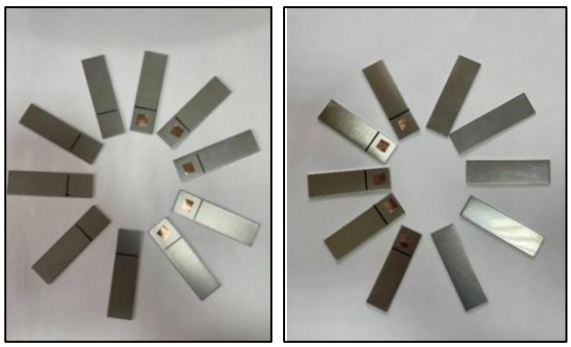

Fig. 4. Samples prepared for welding stainless steel sheets with and without intermediate Cu plate

Table 3. Chemical composition of materials prepared for resistance spot welding [wt%]

Material	C	Si	Mn	P	S	Cr	Ni	Fe	Cu	N	Sn
E304	0.07	1	2	0.045	0.015	17.5-19.5	8-10.5	Bal	-	0,1	-
Cu99	-	0.19	0.22	0.001			<0.01	<0.01	Bal	-	0.674

2.2. Equipment and Methods

The two welded types of joints investigated in this paper, SS-SS and SS-Cu-SS, were resistance spot welded with the same welding parameters. The resistance spot welding equipment used is PPLU-63 with an installed power of 63KVA. The copper electrodes used have a conical tip and a diameter of the active surface of 4.5mm. The two types of welded joints were subjected to tensile testing in order to determine the influence of the copper foil interlayer on their strength.

Simufact Welding software has been used for the modelling and simulation of the resistance spot welding process. The thermal field distribution, in the case of resistance spot welding, depends on the primary welding parameters (amperage, voltage, and welding time); on the thermo-physical properties of the base material (thermal conductivity, specific heat, thermal diffusivity, density); and heat loss that occurs during the process through convection and radiation.

The 3D finite element model consists of two stainless steel plates (80x25x1mm), a copper plate (10x10x0.1mm), and two welding electrodes (copper electrodes, B0-13-18-30-5-31, according to ISO 5821), as shown in figures 5 and 6.

The type of finite element used in the analysis is SOLID7, a three-dimensional parallelepiped isoparametric element with eight nodes, recommended for a thermo-structural analysis.

In order to obtain accurate values of the thermal field, stress, and deformation in the areas of the welded joint, special attention has been given to the mesh size.

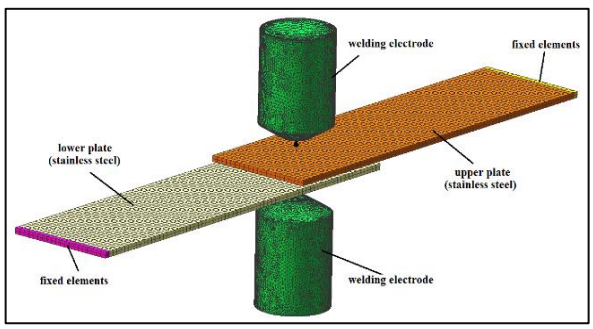

Fig. 5. Finite element model without copper plate intermediate (SS-SS)

The meshed geometrical model constructed for simulation consists of 5680 elements in the case of the joints without the copper intermediate plate. Then it increases to 5770 elements for the joints where the copper foil interlayer is added.

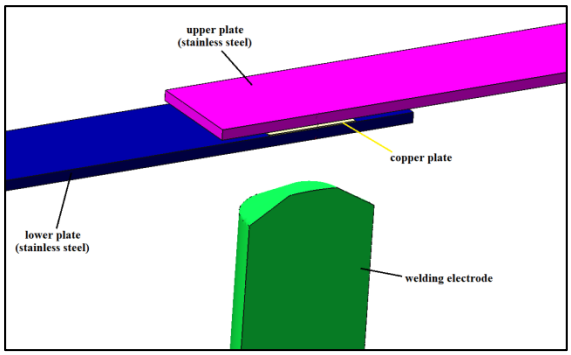

Fig. 6. Finite element model with copper plate intermediate (SS-Cu-SS)

3. RESULTS AND DISCUSSIONS

3.1. Tensile test

The welded samples were subjected to the yield tensile test, and a drop in the resistance of those with the intermediate copper foil was observed from a medium value of 3.43kN breaking load to 2.82kN (Fig. 7). This tendency of decrease in strength of the resistance spot welded joints with Cu foil interlayer was also observed by Dharaiya V. [22], and it is caused by the fact that the copper sheet dissipates the heat generated during the welding process. Therefore, optimization of the welding parameters is needed in order to compensate for the influence of the copper foil interlayer.

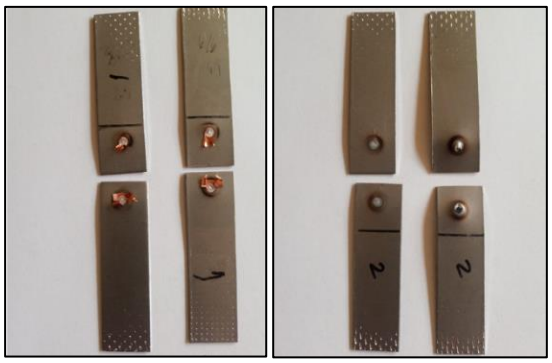

Fig. 7. Tensile test of the welded joints

3.2. Temperature Field

The optimization was made using finite element analysis. After a series of tests, it was concluded that an increase of current amperage from 4.000A to 4.500A is needed so that the weld metal pool forms at the appropriate location between the stainless steel sheets and has an adequate geometry (Fig. 8).

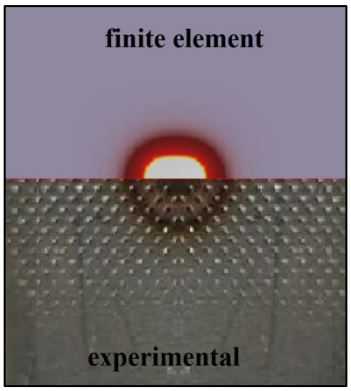

Fig. 8. Validation of the finite element analysis

The results obtained from the finite element analysis were interpreted from the point of view of the thermal field distribution, maximum temperatures, stresses, and deformations in the welded joint. A comparative study of the results was made in the case of resistance spot welding of stainless steel sheets both without a copper intermediate plate and a 4000A welding current and with a copper foil interlayer and a 4500A welding current.

The distribution of the thermal fields in the two cases is presented in figures 9 and 10. It can be observed that in the case of welding with a copper plate interlayer, the diameter of the molten metal core increases from 2 mm to 2.4 mm. This phenomenon is caused by the heat dissipation generated by the Cu foil. The increase in the diameter of the molten metal pool, observed during the FEM analysis, would lead to an improvement in the welded joint strength due to a larger contact surface. The experimental verification of this hypothesis will be done in other studies.

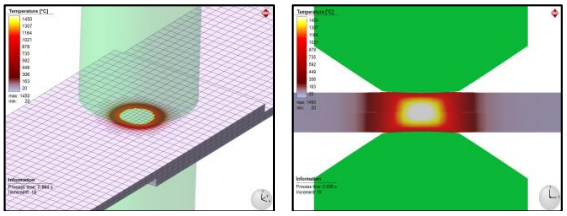

Fig. 9. Thermal field distribution (SS-SS)

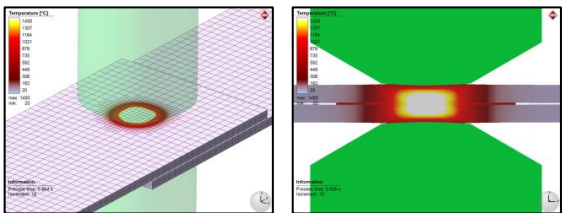

Fig. 10. Thermal field distribution (SS-Cu-SS)

As can be seen in figure 11, twelve nodes were considered on the bottom plate, in order to record the temperatures and effective stress values of the welded joint, as well as in the adjacent areas.

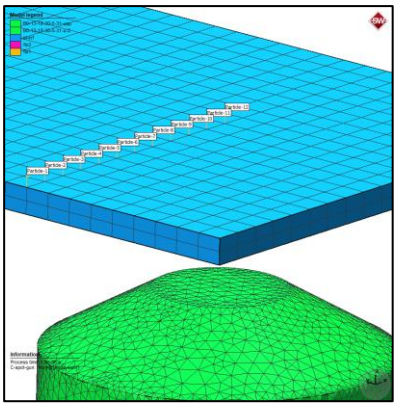

Fig. 11. Positions of the nodes in which the thermal cycles have been analysed

In figure 12, the distribution of temperatures in the considered nodes can be seen. The shape of the graphs is similar, with the difference appearing in the area of maximum temperatures, the higher value, with approximately 25%, being recorded in the case of welding stainless steel plates without a copper plate. This can be explained by the fact that the copper plate has the role of dissipating the heat produced during the welding process, over a larger area.

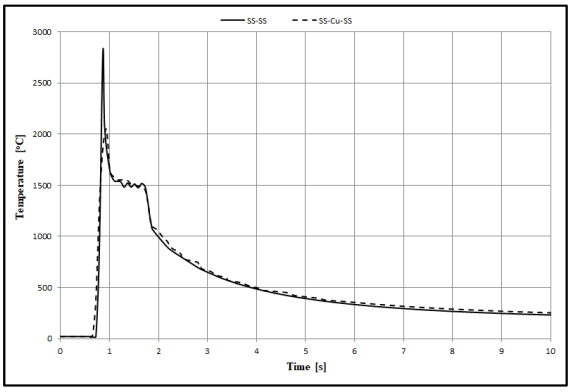

Fig. 12. Thermal history in the welded joint

3.3. Effective stresses

The effective stresses that occur during the welding process have a crucial role in determining the mechanical resistance of the welded joint. In Figures 13 and 14, the effective stress distributions for the two considered cases can be seen both in the isometric view and in the section.

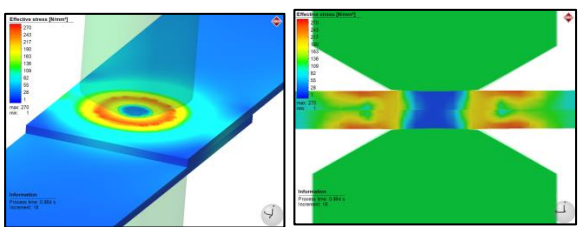

Fig. 13. Effective stresses distribution (SS-SS)

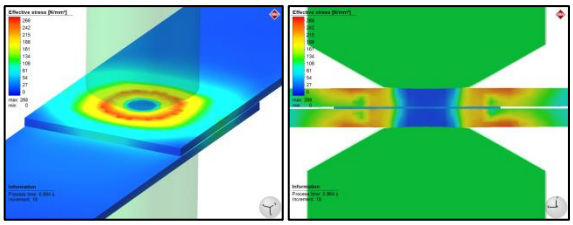

Fig. 14. Effective stresses distribution (SS-Cu-SS)

The graphs of the effective stresses during the welding processes, in the two cases, at the considered points, have similar shapes. The difference between them is negligible, as can be seen in figure 15.

The residual stresses resulting from the welding process are around 480 N/mm^2, which can be reduced by applying a thermal or mechanical treatment.

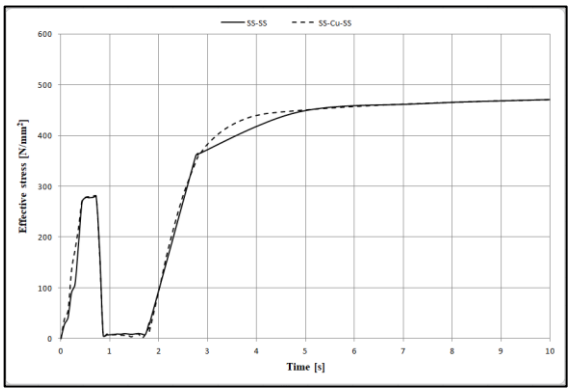

Fig. 15. Effective stress history in the welded joint

4. CONCLUSIONS

The purpose of this study was to investigate the influence of adding a 0.1mm thin copper foil interlayer in resistance spot welding of 1 mm thick E304 stainless steel sheets and the following conclusions can be drawn:

- the copper foil interlayer dissipates a part of the heat that is used for resistance spot welding;
- at the same welding parameters, the joints with a copper foil interlayer had a lower resistance than the ones without one;
- based on the FEM analysis observation, when using a copper foil interlayer, there is a need to increase the current amperage from 4000A to 4500A to compensate for the heat dissipation;
- analysing the thermal field of the FEM simulation, it was observed an increase in the molten metal core diameter, from 2 mm in the SS-SS joint to 2.4 mm in the SS-Cu-SS joint;
- the effective stress analysis shows no significant difference between the two cases investigated, so it can be concluded that the addition of a copper foil interlayer had no influence on the internal stress of the welded joint.

REFERENCES

[1]. **Yu J., Zhang H., Wang B., Gao C., Sun Z., He P.**, *Dissimilar Metal Joining of Q235 Mild Steel to Ti6Al4V via Resistance Spot Welding with Ni–Cu Interlayer*, Journal of Materials Research and Technology 2021, vol. 15, pp. 4086–4101, doi:10.1016/j.jmrt.2021.10.039.

[2]. **Chen T., Ling Z., Wang M., Kong L**., Effect of Post-Weld *Tempering Pulse on Microstructure and Mechanical Properties of Resistance Spot Welding of Q&P1180 Steel*, Materials Science and Engineering: A 2022, vol. 831, 142164, doi:10.1016/j.msea.2021.142164.

[3]. **Brizes E., Jaskowiak J., Abke T., Ghassemi-Armaki H., Ramirez A.J.,** *Evaluation of Heat Transfer within Numerical Models of Resistance Spot Welding Using High-Speed Thermography, Journal of Materials Processing Technology 2021*, vol. 297, 117276, doi:10.1016/j.jmatprotec.2021.117276.

[4]. **Figueredo B., Ramachandran D.C., Macwan A., Biro E.**, *Failure Behavior and Mechanical Properties in the Resistance Spot Welding of Quenched and Partitioned (Q&P) Steels*, Weld World 2021, vol. 65, pp. 2359–2369, doi:10.1007/s40194-021-01179-z.

[5]. **Banga H.K., Kalra P., Kumar R., Singh S., Pruncu C.I.**, *Optimization of the Cycle Time of Robotics Resistance Spot Welding for Automotive Applications*, Journal of Advanced Manufacturing and Processing; Process 2021, vol. 3, doi:10.1002/amp2.10084.

[6]. **Cai W., Daehn G., Vivek A., Li J., *Khan H.*, *Mishra R.S.*, *Komarasamy M.***, *A State-of-the-Art Review on Solid-State Metal Joining*, Journal of Manufacturing Science and Engineering 2019, vol. 141, 031012, doi:10.1115/1.4041182.

[7]. **Zhao D., Ivanov M., Wang Y., Liang D., Du W.**, *Multi-Objective Optimization of the Resistance Spot Welding Process Using a Hybrid Approach*, Journal of Intelligent Manufacturing 2021, vol. 32, pp. 2219–2234, doi:10.1007/s10845-020-01638-2.

[8]. **Deng L., Li Y., Cai W., Haselhuhn A.S., Carlson B.E**, *Simulating Thermoelectric Effect and Its Impact on Asymmetric Weld Nugget Growth in Aluminum Resistance Spot Welding*, Journal of Manufacturing Science and Engineering 2020, vol. 142, 091001, doi:10.1115/1.4047243.

[9]. **Amaral F.F., Almeida F.A., Costa S.C., Leme R.C., Paiva A.P**., *Application of the Response Surface Methodology for Optimization of the Resistance Spot Welding Process in AISI 1006 Galvanized Steel*, Soldagem e Inspecao. 2018, vol. 23, pp. 129–142, doi:10.1590/0104-9224/si2302.02.

[10]. *** MSC.Software GmbH. .Simufact Engineering 2022.

[11]. **Voiculescu I., Geanta V., Stefanescu E.V., Simion G., Scutelnicu E**., *Effect of Diffusion on Dissimilar Welded Joint between Al0.8CoCrFeNi High-Entropy Alloy and S235JR Structural Steel*, Metals 2022, vol. 12, 548, doi:10.3390/met12040548.

[12]. **Birsan D. C., Simion G., Voiculescu I., Scutelnicu E.**, *Numerical Model Developed for Thermo-Mecahnical Analysis in AlCrFeMnNiHf0.05–Armox 500 Steel Welded Joint*, AWET 2021, vol. 32, pp. 37–46, doi:10.35219/awet.2021.05.

[13]. **Mitru A., Semenescu, A., Simion G., Scutelnicu E., Voiculescu I.**, *Study on the Weldability of Copper—304L Stainless Steel Dissimilar Joint Performed by Robotic Gas Tungsten Arc Welding*, Materials 2022, vol. 15, 5535, doi:10.3390/ma15165535.

[14]. **Senthil Murugan S., Sathiya P., Noorul Haq, A**., *Rotary Friction Welding and Dissimilar Metal Joining of Aluminium and Stainless Steel Alloys*, AWET 2021, 32, 85–92, doi:10.35219/awet.2021.11.

[15]. **Scutelnicu E., Simion G., Rusu C. C., Gheonea M. C., Voiculescu I., Geanta V.,** *High Entropy Alloys Behaviour During Welding*, Revista de Chimie, 2001, vol. 71, pp. 219–233, doi:10.37358/RC.20.3.7991

[16]. **Wang T., Zhang B., Feng J., Tang Q.**, *Effect of a Copper Filler Metal on the Microstructure and Mechanical Properties of Electron Beam Welded Titanium–Stainless Steel Joint*, Materials Characterization 2012, vol. 73, pp. 104–113, doi:10.1016/j.matchar.2012.08.004.

[17]. **Zhang B., Wang T., Chen G., Feng J.**, *Contact Reactive Joining of TA15 and 304 Stainless Steel Via a Copper Interlayer Heated by Electron Beam with a Beam Deflection*, Journal of Materials Engineering and Performance 2012, vol. 21, pp. 2067–2073, doi:10.1007/s11665-012-0132-4.

[18]. **Hao X., Dong H., Yu F., Li P., Yang Z.,** *Arc Welding of Titanium Alloy to Stainless Steel with Cu Foil as Interlayer and Ni-Based Alloy as Filler Metal*, Journal of Materials Research and Technology 2021, vol. 13, pp. 48–60, doi:10.1016/j.jmrt.2021.04.054.

[19]. **Eroglu M., Khan T.I., Orhan N.**, *Diffusion Bonding between Ti -6Al -4V Alloy and Microduplex Stainless Steel with Copper Interlayer*, Materials Science and Technology 2002, vol. 18, pp. 68–72, doi:10.1179/026708301125000230.

[20]. **Roudbari M., Refahati N., Mehdipour Omrani A.**, *Production of steel 1006 wire reinforced aluminium base composite by explosive welding*, Revista de Metalurgia, 2020, vol. 56, iss. 165, pp.1-6, doi:10.3989/revmetalm.165.

[21]. **Zhang, W.; Ao, S.; Oliveira, J.P.; Li, C.; Zeng, Z.; Wang, A.; Luo, Z.** *On the Metallurgical Joining Mechanism during Ultrasonic Spot Welding of NiTi Using a Cu Interlayer*. Scripta Materialia, 2020, vol. 178, pp. 414–417, doi:10.1016/j.scriptamat.2019.12.012.

[22]. **Dharaiya V., Panchal A., Acharya G.D**., *Investigating Feasibility of Interlayers in Resistance Spot Welding of Low-Carbon Steel Sheets*, SN Applied Sciences 2021, vol. 3, iss. 749, doi:10.1007/s42452-021-04730-1.

[23]. **Mocanu C. I., Tudose D. I., Hadar A., Gavan E.,** *Strains and Stresses at Welding with Tubular Wires and Swinging the Electric Arc*, IOP Conference Series: Materials Science and Engineering, 2022, 1262, doi:10.1088/1757-899X/1262/1/012053.